Toward Drowsiness Detection Using Non-hair-Bearing EEG-Based Brain-Computer Interfaces

Chun-Shu Wei, *Student Member, IEEE*, Yu-Te Wang, *Member, IEEE*, Chin-Teng Lin, *Fellow, IEEE*, and Tzyy-Ping Jung, *Fellow, IEEE*

***Abstract*— Drowsy driving is one of the major causes that lead to fatal accidents worldwide. For the past two decades, many studies have explored the feasibility and practicality of drowsiness detection using electroencephalogram (EEG)-based brain-computer interface (BCI) systems. However, on the pathway of transitioning laboratory-oriented BCI into real-world environments, one chief challenge is to obtain high-quality EEG with convenience and long-term wearing comfort. Recently, acquiring EEG from non-hair-bearing (NHB) scalp areas has been proposed as an alternative solution to avoid many of the technical limitations resulted from the interference of hair between electrodes and the skin. Furthermore, our pilot study has shown that informative drowsiness-related EEG features are accessible from the NHB areas. This study extends the previous work to quantitatively evaluate the performance of drowsiness detection using cross-session validation with widely studied machine-learning classifiers. The offline results showed no significant difference between the accuracy of drowsiness detection using the NHB EEG and the whole-scalp EEG across all subjects ($p = 0.31$). The findings of this study demonstrate the efficacy and practicality of the NHB EEG for drowsiness detection and could catalyze explorations and developments of many other real-world BCI applications.**

***Index Terms*— Brain-computer interfaces (BCI), electroencephalogram (EEG), non-hair-bearing electrodes, drowsiness.**

I. Introduction

DROWSY driving is one of the major factors that lead to collisions, injuries, or even fatalities [1]. Developing reliable approaches to detect drowsiness during driving is one of the high priority issues for life safety. For the past two decades, many studies have explored the feasibility and practicality of drowsiness detection using electroencephalogram (EEG), the most practical non-invasive modality featuring high temporal resolution and low cost among various types of brain monitoring modalities [2]–[7]. In 1993, Makeig and Inlow [2] have investigated and quantified the correlation between EEG features and task performance (the error rate of detecting above-threshold auditory target stimuli). Subsequent work by Jung *et al.* [3] demonstrated the feasibility of estimating alertness based solely on the variations of EEG spectral power in an auditory monitoring task. They proposed to build a predictive model using the EEG data collected in a training session, and then applied the model to the EEG recorded in a testing session from the same participant to continuously estimate the alertness level.

Based on the correlation between EEG spectra and drowsiness, several studies have contributed to developing algorithms that can estimate the performance of sustained-attention tasks [4]–[7], which have solidified the practicality of a brain-computer interface (BCI) that tracks neurocognitive drowsiness continuously. Although the aforementioned studies have demonstrated the detectability of drowsiness-related EEG markers, their results were obtained with whole-scalp EEG systems in well-controlled laboratory environments. Whether or not the EEG-based drowsiness detection method is practical in real-world environments remains unclear. Applying EEG measurements for monitoring changes of brain cognitive states has been known as one of the grand challenges because of various limitations existing in current EEG recording modalities [8], [9]. In general, EEG acquisition for real-world applications requires following features [10], [11]: 1) Portability, 2) Convenience and long-term wearing comfort, and 3) Acceptable signal quality. The conventional laboratory-oriented EEG recording methodology failed to meet aforementioned requirements because of the use of wet electrodes and conductive gels for reducing the impedance and tethered wires for connecting the computer systems. Furthermore, skin/scalp preparation and cleaning are both time-consuming and inconvenient before and after each EEG recording session. The recent advance in developing portable and wireless EEG recording devices has made significant improvements in terms of portability and convenience of EEG [12]–[14]. Nonetheless, dry-electrodes still face difficulty in achieving stable electrode-skin contact in hair-covered scalp areas

Manuscript received October 5, 2016; revised July 31, 2017 and November 2, 2017; accepted December 18, 2017. Date of publication January 5, 2018; date of current version February 9, 2018. This work was supported in part by the Army Research Laboratory through the Cooperative Agreement under Grant W911NF-10-2-0022 and Grant W911NF-10-D-0002/TO 0023 and in part by the Australian Research Council under Grant DP180100670 and Grant DP180100656. *(Corresponding author: Tzyy-Ping Jung.)*

C.-S. Wei is with the Department of Bioengineering, Jacobs School of Engineering, with the Swartz Center for Computational Neuroscience, Institute for Neural Computation, and also with the Center for Advanced Neurological Engineering, Institute of Engineering in Medicine, UCSD, La Jolla, CA 92093 USA (e-mail: cswei@sccn.ucsd.edu).

Y.-T. Wang and T.-P. Jung are with the Swartz Center for Computational Neuroscience, Institute for Neural Computation, and also with the Center for Advanced Neurological Engineering, Institute of Engineering in Medicine, UCSD, La Jolla, CA 92093 USA (e-mail: yute@sccn.ucsd.edu; jung@sccn.ucsd.edu).

C.-T. Lin is with the Centre for Artificial Intelligence, FEIT, University of Technology Sydney, City Campus, Sydney, NSW 2007, Australia (e-mail: chin-teng.lin@uts.edu.au).

Digital Object Identifier 10.1109/TNSRE.2018.2790359

without conductive gels. To reduce the interference from the hair between electrodes and the skin, current dry electrodes often used pins, either solid or flexible, to penetrate the hair layer [12]–[14]. According to a previous study on user experience of dry electrodes, even soft-pin-based electrodes could cause erythema after long-term applications [15]. Overall, in terms of portability, convenience, long-term wearing comfort, and acceptable signal quality, none of the existing EEG recording devices has met all of the requirements for real-world use. However, even though the EEG recording devices might not have a satisfactory solution for real-world use immediately, there might be a compromise solution. Lately, a non-hair-bearing (NHB) montage that measures EEG signals from frontal, ear, mastoid, and neck areas has been proposed for measuring EEG signals in real-world BCI applications, because it avoids the interference of electrode-skin contact caused by the hair [16]–[20]. Generally speaking, the NHB BCI uses only easily accessible areas of the scalp, and could be realized with EEG recording devices featuring minimal weight and size, which are necessary for portability, convenience of use and long-term wearing comfort. Furthermore, without the interference from the hair, the relatively stable skin-electrode contact could improve the convenience of recording setup without the use of conductive gels or pin-shaped electrodes. Recently, steady-state visual evoked potential (SSVEP) detection based on the NHB EEG has been validated and applied in a BCI speller [20]. The online performance of the NHB SSVEP speller could reach 30 bit/min using solely the mastoid areas. Another potential use of NHB EEG is drowsiness detection. In our pilot study, we have demonstrated accessing EEG features associated with neurocognitive drowsiness from the NHB EEG, and those NHB EEG features could achieve the comparable efficacy of discriminating trials with short vs. long response time (RT) in response to lane-departure events to the whole-scalp EEG [21].

This study aims to comprehensively investigate and validate the feasibility of using the NHB EEG as biomarkers for continuous tracking and detection of neurocognitive drowsiness. First, we assessed the drowsiness-related information available in the EEG by a comparison between the EEG correlates of drowsiness from the whole-scalp and those from the NHB channels. Next, we used the drowsiness-related NHB EEG features to develop a framework for drowsiness detection, and compare the performance of classification using the NHB EEG with that of using the whole-scalp EEG. Finally, we validated the performance of the proposed NHB montage for drowsiness detection with cross-session validation on 10 subjects preforming lane-keeping driving experiments.

II. Method

A. Experiment

This study scrutinizes EEG correlates of drowsiness during a lane-keeping driving experiment [22]. The experiment took place in a realistic virtual-reality (VR) driving simulator that created immersed driving experience for the participants. The VR driving simulator was composed of an authentic coupe car body mounted on a 6-degree-of-freedom motion platform and surrounding projector screens playing driving scene. During the experiment, a subject was sitting in the driver seat while the car automatically cruised forward at the speed of 100 km/h on a nighttime straight highway. During the experiment, lane-departure events were repeatedly introduced every 6-10 seconds, in which the car drifted toward either left or right randomly, and the participant was instructed to steer the car back to the course once he/she was aware of the lane-departure events. The point in time when the lane-departure event occurred, when the subject responded to the lane-departure event, and when the subject finished steering the car back to the course, were logged as deviation onset, movement onset, and movement offset, respectively. The experiment started after lunch and lasted for ∼90 min in order to maximize the chance of drowsy driving by afternoon slump [23]. Ten subjects with normal or corrected-to-normal vision participated in the experiment, and each of them performed two sessions on different days. The experiment was approved by the Institutional Review Board of the Veterans General Hospital, Taipei, Taiwan. All participants were asked to read and sign an informed consent form before the EEG experiment. For the details of the participants and the experiment, readers are referred to [7].

B. Evaluation of Neurocognitive Drowsiness

In the lane-departure event, the level of drowsiness in that given moment was quantitatively estimated based on the RT, which defined as the time between the deviation onset and the wheel-steering onset. For each subject, the RT in each lane-departure event was named local RT, which represents the short-term level of drowsiness. On the other hand, the long-term level of drowsiness was defined by global RT, which was calculated by averaging the RTs across all trials within a 90-second window before the onset of the deviation [5]. For each driving session, the 'alert RT' was measured as the 5^{th} percentile of local RTs across the entire session, representing the RT that the subject could perform during alertness. Trials with both local and global RT shorter than 1.5 times alert RT were categorized as 'alert' trials, whereas those with both local and global RT longer than 2.5 times alert RT were labeled as 'drowsy' trials. Such a categorization excluded the transitioning trials that correspond to a moderate performance of the driver, since intermediate RT might be attributed to other unknown processes, e.g. mind-wandering, and the exclusion of transitioning trials could benefit the accuracy of discriminating drowsy trials [7], [21]. The total numbers of alert, transitioning, and drowsy trials were 2,940, 4,506, and 1,512, respectively, across 10 subjects. This study focuses on the detection of drowsiness (low performance) where interventions are necessary by training our machine-learning classifiers with well-defined alert vs. drowsy trials.

C. EEG Recording and Processing

In the experiment, the EEG activity of each subject was recorded using a 32-channel Quik-Cap (Compumedics NeuroScan Inc.) following the International 10-20 system of electrode placement with Ag/AgCl gel-based electrodes.

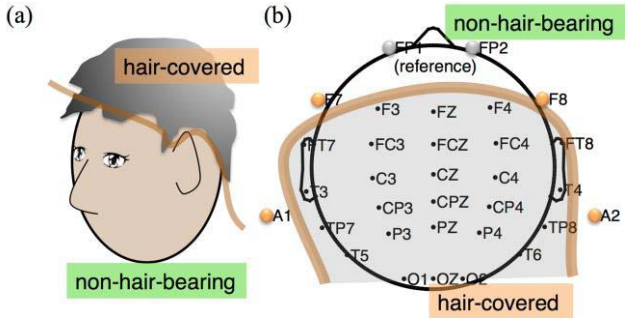

Fig. 1. (a) The partition of hair-covered areas and non-hair-bearing area divided by a brown boundary. (b) The layout of electrode locations of the 32-channel recording system. Brown boundary separates the divisions of hair-covered and non-hair-bearing area.

The raw EEG signals were sampled at 500 Hz with 16-bit quantization. Six electrodes, Fp1, Fp2, F7, F8, A1, and A2 were placed on NHB areas (see Fig. 1). All EEG data were re-referenced to the arithmetic average of Fp1 and Fp2. F7, F8, A1, and A2 were noted as the NHB channels for further analysis. To be specific, F7 and F8 measured the brain activity in the frontal area, while A1 and A2 recorded the brain activity in the left and right mastoid areas, respectively. The EEG signal of each channel underwent a 1-50 Hz band-pass finite impulse response filter to remove low-frequency DC drifts and power line noise at 60 Hz. The filtered EEG data were then down-sampled to 250 Hz to reduce computational load. The data were then cleaned by the procedure of artifact subspace reconstruction (ASR) [24] provided in EEGLAB [25]. The ASR detects high-variance signal components above a given threshold and linearly reconstructed by the retained uncontaminated signal subspace based on principal component analysis of 1-min calibration data [26].

D. EEG Feature Extraction and Assessment

The EEG features related to neurocognitive drowsiness have been investigated in numbers of previous studies [2]–[6], [27], [28], and have been extended into BCI applications for predicting the human performance in a sustained attention task [3], [5], [27], [28]. As suggested in the preliminary study [21], we employed the EEG data prior to the onset of the task event as features for building a predictive model that can continuously estimates the performance index without relying on any EEG activities induced by infrequent and unexpected events. In this study, theta (4-8 Hz), alpha (8-13 Hz), and beta (13-30 Hz) logarithmic powers of 3s-long pre-event EEG before each lane-departure event were exploited for classifying the 'alert' vs. 'drowsy' on the upcoming lane-departure event [21]. For each trial, the logarithmic powers of the 3-s pre-lane-departure sub-band-passed EEG segments were estimated. Then, the sub-band logarithmic powers were smoothed to eliminate unrelated spectral perturbations. Finally, both the unsmoothed and smoothed pre-event logarithmic theta, alpha and beta powers for all-channel (AC)/NHB channels congregated a 180/24-dimensional feature set for drowsiness detection. Essentially, the AC montage represents the conventional whole-scalp BCI setting that includes EEG data acquired from both the hair-covered and the NHB areas. A series of analyses and classification experiments was performed in order to quantitatively assess and compare the validity of drowsiness detection based on the AC and the NHB montages.

E. Classifiers

Three classic classification methods, linear discriminant analysis (LDA), k nearest neighbors (kNN) and support vector machine (SVM) that have been widely used in EEG classification were employed in this study to discriminate the EEG activity of drowsy state from that of alert state.

1) Linear Discriminant Analysis: LDA aims to project data onto hyperplanes for maximizing the separation between data from different classes while minimizing the variance of data within the same class [29]. According to statistics, LDA is the most commonly used classification method in BCI studies [30]. Because of its low computational requirement and efficiency, LDA is an ideal simple tool to perform classification for online BCI systems. Nonetheless, the simplicity of LDA is also its drawback as it could fail in dealing with non-linear EEG data [31]. We applied the conventional LDA combined with maximal likelihood (ML) classification that has been used in the preliminary study [21].

2) k Nearest Neighbors: The kNN classifier is a non-parametric instance-based approach for classifying a sample in the feature space [32]. In the kNN classification, the class of a sample is determined by a majority vote of its k neighboring samples. However, kNN algorithms are known for their sensitivity to curse-of-dimensionality, and are not as widely used in BCI researches as LDA or SVM [31]. We included kNN in this study for the sake of diversity of classic classifiers, where $k = 5$ has been pre-optimized empirically.

3) Support Vector Machine: SVM is the second most used classifier in BCI studies [30]. Analogous to LDA, SVM also maps data upon a hyperplane, whereas it selects the hyperplane that maximizes the margin between different classes [33]. One advantage of SVM is the generalizability resulted from margin maximization that prevents over-fitting and curse of dimensionality [31], which is crucial for classifying EEG data. The flexibility of kernel selection allows SVM to handle complex data, but optimizing the parameters could be a time-consuming task. In this study, we used LIBSVM [34] with a linear kernel and grid-search optimization on 5-fold cross validation. The SVM classifier has been used in previous BCI applications for real-time EEG classification [35], [36].

III. Results

Fig. 2 shows the topographical distribution of Pearson correlation coefficients between normalized RT [35] and the pre-event EEG power at different frequency bands. In particular, strong EEG correlates of RTs could be found in the frontal theta (negative correlation) and parietal-occipital alpha (positive correlation). The broad distribution of strong EEG correlates (red and blue on the scalp topography) suggests that the informative drowsiness-related EEG dynamics could be extracted from both the hair-covered and the NHB areas.

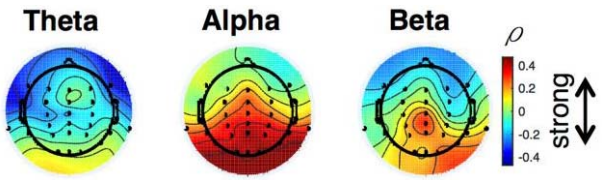

Fig. 2. The scalp topography of correlation distributions that exhibits the correlation coefficients (ρ) between normalized RT and pre-event EEG power features of theta, alpha, and beta band at different channel locations across subjects. Strong drowsiness-correlated EEG dynamics, particularly at frontal theta and parietal-occipital alpha, disperse across whole scalp, including both hair-cover and NHB areas.

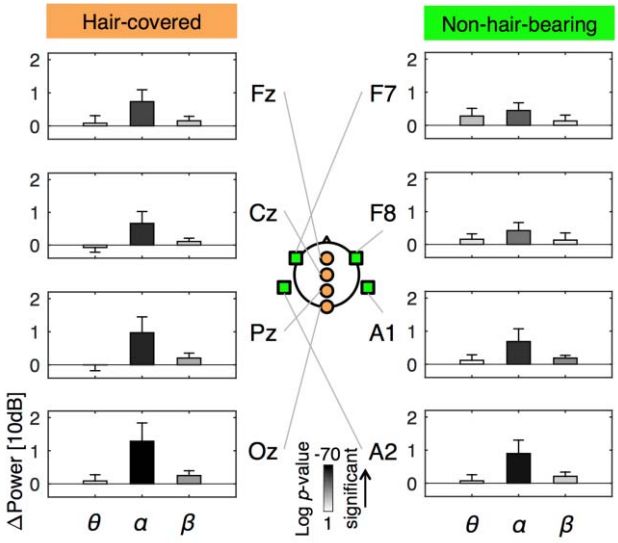

Fig. 3. EEG spectral changes from alertness to drowsiness at different representative channels and frequency bands. Bar plots illustrate the average increments across subjects of band power from the alert state to the drowsy state, and error bars mark standard deviations. The spectral increment for each band is calculated by averaging the logarithmic band powers of the 3-s pre-lane-departure EEG across all trials from the drowsy state, and subtracted by the mean logarithmic band power of alert trials. The gray scale filled in each bar indicates the *p*-value of two-sample *t*-test for the significance of the difference between the average log-powers of alert and drowsy states. In the left column, Fz, Cz, Pz, and Oz are four representative channels selected from the hair-covered areas, while in the right column, F7, F8, A1, and A2 are four NHB channels utilized for drowsiness detection. Although the increments of powers are larger at the hair-covered channels than those at the NHB channels, both hair-covered and NHB channels exhibited highly significant power increases in the alpha band.

To validate the significance of drowsiness-related EEG features in the NHB areas, the spectral changes of pre-event EEG between short-RT and long-RT trials at the NHB channels were compared with those at the selected hair-covered channels in Fig. 3. The statistical analysis indicates strong discriminative features, in particular at the alpha band in both the hair-covered and NHB areas. Table I summarizes the spectral differences in pre-event EEG between alert and drowsy state. Though the spectral differences of the NHB EEG between short- and long-RT trials were slightly weaker than those of hair-covered EEG (at Oz), the NHB EEG features are comparable to hair-cover EEG features in the statistical strength of discriminating drowsy state from alert state, which supports the feasibility of using NHB EEG to detect drowsiness.

TABLE I
POWER DIFFERENCE OF EEG FEATURES BETWEEN ALERT AND DROWSY STATE

		Δ Power (dB)		
	Channel	Theta	Alpha	Beta
Hair-covered	Fz	0.82±2.30	**7.33±3.61**	**1.54±1.37**
	Cz	**-0.74±1.45**	**6.60±3.67**	**1.08±1.03**
	Pz	-0.01±1.78	**9.71±4.82**	**2.05±1.51**
	Oz	0.87±1.88	**12.88±5.56**	**2.50±1.48**
NHB	F7	**2.79±2.36**	**4.47±1.77**	**1.33±1.77**
	F8	**1.59±1.66**	**4.24±2.21**	**1.33±2.21**
	A1	1.19±1.68	**6.87±3.88**	**1.87±0.82**
	A2	0.73±3.88	**8.98±4.07**	**2.10±1.29**

Bold: $p<0.001$, two-sample *t* test.

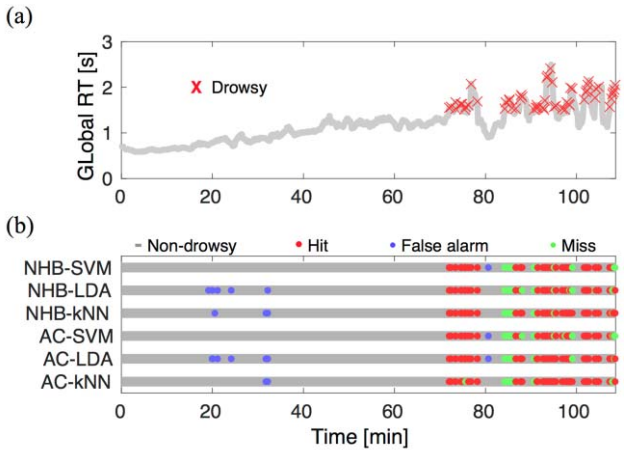

Fig. 4. (a) The change of global RT across an entire session of subject 9. Gray line shows the interpolated global RT using the global RT of neighboring trials. Red cross indicates the events that are labeled as 'drowsy'. (b) The classification results of drowsiness detection using three types of classifier (SVM, LDA, and kNN) with NHB and AC EEG for the same session as in (a). Hits, false alarms, and misses were marked as red, blue, and green dots, respectively. Note that drowsiness detection was performed only at the time right before a lane-departure event presents. The non-drowsy outcome was denoted as a gray belt, which includes the 'alert' predictions and other non-drowsy intervals, such as cruise driving and wheel-steering.

Fig. 4 shows the performance of drowsiness detection for a sample session (second session of subject 9, S9-2). Fig. 4(a) illustrates the fluctuations of global RTs during the entire driving session, where red crosses mark drowsy trials. The driving performance of S9 in the session gradually declined and entered a drowsy state ~70 minutes on the task. Fig. 4(b) exhibits the prediction of alert/drowsy trials of this session. In the first half of the session, NHB-SVM and AC-SVM have successful classified the EEG spectra without any false alarm, whereas LDA and *k*NN classifiers both made some erroneous classifications. From ~70 minute onwards, all approaches detected drowsiness at the transition point of the subject's neurocognitive state. In the later part of the session, as the subject's state shifted back and forth between drowsiness and alertness, all these classifiers predicted drowsy trials correctly, and erroneous predictions tend to occur during the transitions between states. The ROC curves of drowsiness detection of the sample session (S9-2) using the LDA and the SVM were compared in Fig. 5.

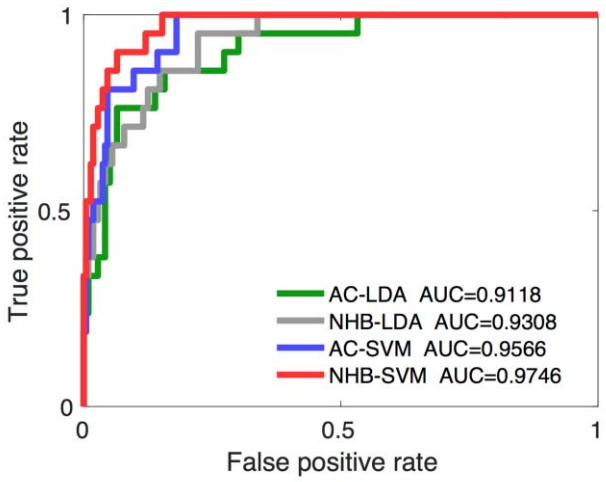

Fig. 5. ROC curves describing the relation between true positive rate (sensitivity) and false positive rate (specificity) using NHB EEG and AC EEG with different classifiers on subject 9. Note that positive refers to drowsiness.

TABLE II
OVERALL ACCURACY OF DROWSINESS DETECTION USING WITHIN-SUBJECT CROSS-SESSION VALIDATION

Montage	Accuracy (%)		
	SVM	LDA	*k*NN
NHB	80.0±8.6	79.4±8.7	77.3±10.7
AC	83.3±7.4	78.1±11.9	75.3±12.6

Finally, the performances of alert/drowsy classification obtained by three types of classifier using the NHB EEG and the AC EEG were tested by within-subject cross-session validation. Fig. 6 and Table II compare the averaged accuracies across all subjects using different montages combined with different classifiers. Two-way ANOVA was applied for analyzing 1) the difference among classifiers and 2) the difference between using the NHB and the AC EEG. The test results show no significant difference in the accuracy between using the NHB and the AC EEG, nor among the three classifiers (Two-way ANOVA, $p = (0.31, 0.16)$). Furthermore, the area under the ROC curve (AUC) is jointly employed to evaluate the classification performance and summarized as in Table III. Tested by two-way ANOVA, the overall AUC across subjects presents significant difference between the classifiers ($p < 0.01$) but no significant difference across between the NHB and AC montages ($p = 0.34$).

IV. DISCUSSION

In this study, we proposed using a novel EEG recording montage in NHB areas for future BCI applications featuring convenience, economy, and long-term sustainability. Although the concept of drowsiness-related EEG features in the NHB areas has been proposed in our preliminary study on a small group of subjects, the efficacy of using the NHB EEG for BCI applications remains unclear. We hereby comprehensively validated the performance of drowsiness detection based on the NHB EEG across sessions (days). Furthermore, several widely studied BCI classifiers were employed and compared

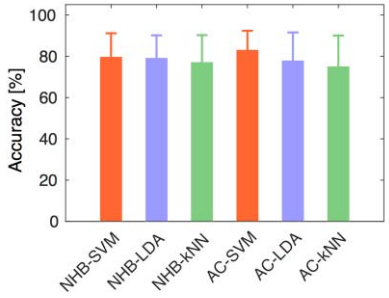

Fig. 6. The bar plot compares the average accuracy of drowsiness detection with standard deviation using different metrics across subjects. No significant difference was found between the NHB and the AC montages, nor among the three classifiers (Two-way ANOVA, p=(0.31, 0.16)).

TABLE III
OVERALL AUC OF DROWSINESS DETECTION USING WITHIN-SUBJECT CROSS-SESSION VALIDATION

Montage	AUC	
	SVM	LDA
NHB	0.8576±0.0753	0.7312±0.1412
AC	0.8759±0.0757	0.7758±0.1041

quantitatively in their performances of drowsiness detection between using the NHB and the whole-scalp montage. Study results suggested that the NHB EEG could provide comparable performance in drowsiness detection to that of the AC EEG regardless of the classifier being used.

A. EEG Correlates of Drowsiness in the NHB Areas

It has been shown that drowsiness-related EEG activities could be assessed from various areas over the scalp [3]–[5], [39]. For instances, EEG correlates of drowsiness have been identified and validated in frontal theta [39] and parietal-occipital alpha [3]–[5]. The experimental results of this study confirmed the topographical distribution of drowsiness-related EEG features (Fig. 2), which plays a key role in facilitating the design and use of the NHB EEG-based drowsiness detection. According to the study results shown in Fig. 3 and Table I, both the NHB and the AC EEG exhibited highly significant spectral differences between alertness and drowsiness. To make a fair comparison on the efficacy of the EEG-based drowsiness detection, we used the same types of electrodes to acquire the AC and NHB EEG simultaneously. This study provides an objective evidence of the feasibility of current and future implications of the NHB EEG.

B. Drowsiness Detection Using the NHB EEG

Although drowsiness-related features of the NHB EEG showed slightly weaker significances in the spectral differences between alertness and drowsiness compared with those of the hair-cover areas (Fig. 3 and Table I), the classification accuracy of drowsiness detection obtained from the NHB EEG is still comparable to that obtained from the AC EEG (Fig. 6, Table II, and Table III). This could be explained by the intrinsically low spatial specificity of EEG recording, which leads to high signal similarity among different

channels [40]. As mentioned above, drowsiness-related brain activity is widely spread across a large scalp area, and thus could be assessable from either the hair-covered areas or the NHB areas. The promising findings could encourage further explorations of BCIs based on the NHB EEG. For instance, based on these experimental results, one could develop an NHB BCI that continuously monitors a driver's cognitive state, and mitigates the driver's drowsiness by delivering arousing feedback or other stimulations during the transitioning from alertness to drowsiness [41], [42]. This study exploited only the pre-event EEG spectra to discriminate alertness vs. drowsiness of the participants, because drowsiness is most likely to occur during monotonous, uneventful driving in real life. It is impractical to use and rely on EEG spectra following lane-departure events, as they might not present frequently in real driving. Therefore the data processing and analysis for validating the performance of drowsiness detection in this study was designed within a real-world scenario with online applicability. Meanwhile, it is intriguing to investigate how early the drowsiness can be detected in the future work. This could be examined by inserting a varying gap between the data being used for classification and the lane-departure event. As the first attempt made for monitoring human cognitive state related to driving performance using the NHB BCI, the extensions of this study could emerge for other tasks that require maintenance of continuous attention [43].

C. Advantages of NHB EEG for Real-World BCI

As the recording area is smaller than using the whole scalp, the wearable device for NHB BCIs is expected to be lighter, more portable, and easier to wear. In addition, the cost of small number of electrodes required for an NHB BCI could is lower than that of a high-density montage. In fact, consumer wearable devices that acquire EEG signals from NHB areas, such as Neurosky XWave [44] and InteraXon Muse [45], have been commercially available, and their prices are considerably lower than that of the commercial products featuring whole-scalp recording such as Emotiv Epoc [46]. Another advantage of using NHB EEG is that the NHB areas are favorable for most dry or semi-dry EEG electrodes since it has low impedance of skin-electrode contact. For instances, dry Ag/AgCl electrodes, disposable paste ECG electrodes, or patch sensors all prefer or require hairless surfaces. In particular, the recent advance of epidermal sensor patches has made long-term biometric measurements possible in the real world with their softness and deformability [17], [47]. The epidermal sensor patches could facilitate maximal comfort in long-term signal acquisition, but are not applicable in the hair-covered areas.

Still, there is a limitation of building a BCI based on the NHB EEG, since most of the EEG activities that have been studied were assessed from hair-covered areas. For certain brain responses that are locally distributed in the central area, the NHB EEG might have low signal-to-noise ratio. Furthermore, as the spatial distributions of brain activities vary across individuals [48], [49], the NHB BCI might face severe challenges in maintaining robustness across individuals. The efficacy of NHB EEG requires further investigations on different types of brain activities. In view of these considerable advantages of using the NHB EEG in real-world applications, there is a need for further explorations on what information are available from the NHB areas and what applications could be facilitated using the NHB EEG.

V. Conclusion

The current study presented the efficacy of using EEG features that are easily accessible from the NHB areas of the scalp for assessing driving drowsiness. To explore the amount of drowsiness-related information available in the NHB EEG, we quantitatively showed that the spectral differences between alertness and drowsiness in the pre-event (lane-deviation) EEG obtained from the NHB areas are slightly weaker than that obtained from the AC areas. Nonetheless, the drowsiness-related information from the NHB EEG was sufficient to provide comparable drowsiness detection accuracy to that of using the information from the whole-scalp EEG. In general, replacing the whole-scalp recording with the NHB montage is an important and practical step toward real-world BCIs, as there are considerable advantages on the efficiency of sensors, the flexibility of mechanical design, and the improvement of user experience. We believe this study will ignite many new real-world BCI applications that can benefit from the convenience and informativeness of the NHB EEG.

References

[1] F. Vaca, J. S. Harris, H. G. Garrison, and M. P. McKay, "Drowsy driving," *Ann. Emerg. Med.*, vol. 45, no. 4, pp. 433–434, 2005.
[2] S. Makeig and M. Inlow, "Lapse in alertness: Coherence of fluctuations in performance and EEG spectrum," *Electroen. Clin. Neurophysiol.*, vol. 86, no. 1, pp. 23–35, Jan. 1993.
[3] T.-P. Jung, S. Makeig, M. Stensmo, and T. J. Sejnowski, "Estimating alertness from the EEG power spectrum," *IEEE Trans. Biomed. Eng.*, vol. 44, no. 1, pp. 60–69, Jan. 1997.
[4] P. Parikh and E. Micheli-Tzanakou, "Detecting drowsiness while driving using wavelet transform," in *Proc. IEEE 30th Annu. Northeast Bioeng. Conf.*, Apr. 2004, pp. 79–80.
[5] C.-T. Lin, R.-C. Wu, S.-F. Liang, W.-H. Chao, Y.-J. Chen, and T.-P. Jung, "EEG-based drowsiness estimation for safety driving using independent component analysis," *IEEE Trans. Circuits Syst. I, Reg. Papers*, vol. 52, no. 12, pp. 2726–2738, Dec. 2005.
[6] R. R. Johnson, D. P. Popovic, R. E. Olmstead, M. Stikic, D. J. Levendowski, and C. Berka, "Drowsiness/alertness algorithm development and validation using synchronized EEG and cognitive performance to individualize a generalized model," *Biol. Psychol.*, vol. 87, no. 2, pp. 241–250, 2011.
[7] C.-H. Chuang, L.-W. Ko, Y.-P. Lin, T.-P. Jung, and C.-T. Lin, "Independent component ensemble of EEG for brain–computer interface," *IEEE Trans. Neural Syst. Rehabil. Eng.*, vol. 22, no. 2, pp. 230–238, Mar. 2014.
[8] M. M. Moore, "Real-world applications for brain–computer interface technology," *IEEE Trans. Neural Syst. Rehabil. Eng.*, vol. 11, no. 2, pp. 162–165, Jun. 2003.
[9] B. Z. Allison, E. W. Wolpaw, and J. R. Wolpaw, "Brain–computer interface systems: Progress and prospects," *Expert Rev. Med. Devices*, vol. 4, no. 4, pp. 463–474, Jul. 2007.
[10] J. Van Erp, F. Lotte, and M. Tangermann, "Brain–computer interfaces: Beyond medical applications," *IEEE Comput.*, vol. 45, no. 4, pp. 26–34, Apr. 2012.
[11] K. Mcdowell *et al.*, "Real-world neuroimaging technologies," *IEEE Access*, vol. 1, pp. 131–149, 2013.
[12] Y. M. Chi, Y.-T. Wang, Y. Wang, C. Maier, T.-P. Jung, and G. Cauwenberghs, "Dry and noncontact EEG sensors for mobile brain–computer interfaces," *IEEE Trans. Neural Syst. Rehabil. Eng.*, vol. 20, no. 2, pp. 228–235, Mar. 2012.

[13] C.-T. Lin, L.-D. Liao, Y.-H. Liu, I.-J. Wang, B.-S. Lin, and J.-Y. Chang, "Novel dry polymer foam electrodes for long-term EEG measurement," *IEEE Trans. Biomed. Eng.*, vol. 58, no. 5, pp. 1200–1207, May 2011.

[14] C. Grozea, C. D. Voinescu, and S. Fazli, "Bristle-sensors—low-cost flexible passive dry EEG electrodes for neurofeedback and BCI applications," *J. Neural Eng.*, vol. 8, no. 2, p. 25008, 2011.

[15] Y.-H. Chen *et al.*, "Soft, comfortable polymer dry electrodes for high quality ECG and EEG recording," *Sensors*, vol. 14, no. 12, pp. 23758–23780, Dec. 2014.

[16] P. Kidmose, D. Looney, M. Ungstrup, M. L. Rank, and D. P. Mandic, "A study of evoked potentials from ear-EEG," *IEEE Trans. Biomed. Eng.*, vol. 60, no. 10, pp. 2824–2830, Oct. 2013.

[17] J. J. S. Norton *et al.*, "Soft, curved electrode systems capable of integration on the auricle as a persistent brain–computer interface," *Proc. Nat. Acad. Sci.*, vol. 112, no. 13, pp. 3920–3925, Mar. 2015.

[18] H.-T. Hsu *et al.*, "Evaluate the feasibility of using frontal SSVEP to implement an SSVEP-based BCI in young, elderly and ALS groups," *IEEE Trans. Neural Syst. Rehabil. Eng.*, vol. 24, no. 5, pp. 603–615, May 2016.

[19] S. Debener, R. Emkes, M. de Vos, and M. Bleichner, "Unobtrusive ambulatory EEG using a smartphone and flexible printed electrodes around the ear," *Sci. Rep.*, vol. 5, Nov. 2015, Art. no. 16743.

[20] Y.-T. Wang, M. Nakanishi, Y. Wang, C.-S. Wei, C.-K. Cheng, and T.-P. Jung, "An online brain–computer interface based on SSVEPs measured from non-hair-bearing areas," *IEEE Trans. Neural Syst. Rehabil. Eng.*, vol. 25, no. 1, pp. 14–21, Jan. 2017.

[21] C.-S. Wei, Y.-T. Wang, C.-T. Lin, and T.-P. Jung, "Toward non-hair-bearing brain–computer interfaces for neurocognitive lapse detection," in *Proc. 37th Annu. Int. Conf. IEEE Eng. Med. Biol. Soc. (EMBC)*, Aug. 2015, pp. 6638–6641.

[22] R.-S. Huang, T.-P. Jung, A. Delorme, and S. Makeig, "Tonic and phasic electroencephalographic dynamics during continuous compensatory tracking," *NeuroImage*, vol. 39, no. 4, pp. 1896–1909, Feb. 2008.

[23] E. A. Mitler and M. M. Merrill, *101 Questions About Sleep and Dreams*. Del Mar, CA, USA: Wakefulness-Sleep Education and Research Foundation, 1988.

[24] T. Mullen *et al.*, "Real-time modeling and 3D visualization of source dynamics and connectivity using wearable EEG," in *Proc. 35th Annu. Int. Conf. IEEE Eng. Med. Biol. Soc. (EMBC)*, Jul. 2013, pp. 2184–2187.

[25] A. Delorme and S. Makeig, "EEGLAB: An open source toolbox for analysis of single-trial EEG dynamics including independent component analysis," *J. Neurosci. Methods*, vol. 134, no. 1, pp. 9–21, Mar. 2004.

[26] C. Kothe. (2013). *The Artifact Subspace Reconstruction Method*. Accessed: Jul. 17, 2017. [Online]. Available: https://sccn.ucsd.edu/eeglab/plugins/ASR.pdf

[27] S. K. L. Lal, A. Craig, P. Boord, L. Kirkup, and H. Nguyen, "Development of an algorithm for an EEG-based driver fatigue countermeasure," *J. Safety Res.*, vol. 34, no. 3, pp. 321–328, Aug. 2003.

[28] M. T. R. Peiris, R. D. Jones, P. R. Davidson, G. J. Carroll, and P. J. Bones, "Frequent lapses of responsiveness during an extended visuomotor tracking task in non-sleep-deprived subjects," *J. Sleep Res.*, vol. 15, no. 3, pp. 291–300, Sep. 2006.

[29] R. A. Fisher, "The use of multiple measurements in taxonomic problems," *Ann. Eugenics*, vol. 7, no. 2, pp. 179–188, Sep. 1936.

[30] H.-J. Hwang, S. Kim, S. Choi, and C.-H. Im, "EEG-based brain–computer interfaces: A thorough literature survey," *Int. J. Hum.-Comput. Int.*, vol. 29, no. 12, pp. 814–826, Dec. 2013.

[31] F. Lotte, M. Congedo, A. Lécuyer, F. Lamarche, and B. Arnaldi, "A review of classification algorithms for EEG-based brain–computer interfaces," *J. Neural Eng.*, vol. 4, no. 2, p. R1, 2007.

[32] D. J. McFarland, C. W. Anderson, K.-R. Müller, A. Schlögl, and D. J. Krusienski, "BCI Meeting 2005-workshop on BCI signal processing: Feature extraction and translation," *IEEE Trans. Neural Syst. Rehabil. Eng.*, vol. 14, no. 2, pp. 135–138, Jun. 2006.

[33] C. J. C. Burges, "A tutorial on support vector machines for pattern recognition," *Data Mining Knowl. Discovery*, vol. 2, no. 2, pp. 121–167, 1998.

[34] C.-C. Chang and C.-J. Lin, "LIBSVM: A library for support vector machines," *ACM Trans. Intell. Syst. Technol.*, vol. 2, no. 3, pp. 27:1–27:27, Mar. 2011.

[35] R. Meier, H. Dittrich, A. Schulze-Bonhage, and A. Aertsen, "Detecting epileptic seizures in long-term human EEG: A new approach to automatic online and real-time detection and classification of polymorphic seizure patterns," *J. Clin. Neurophysiol.*, vol. 25, no. 3, pp. 119–131, Jun. 2008.

[36] L. Chisci *et al.*, "Real-time epileptic seizure prediction using AR models and support vector machines," *IEEE Trans. Biomed. Eng.*, vol. 57, no. 5, pp. 1124–1132, May 2010.

[37] Q. Wang and O. Sourina, "Real-time mental arithmetic task recognition from EEG signals," *IEEE Trans. Neural Syst. Rehabil. Eng.*, vol. 21, no. 2, pp. 225–232, Mar. 2013.

[38] C.-S. Wei, Y.-P. Lin, Y.-T. Wang, T.-P. Jung, N. Bigdely-Shamlo, and C.-T. Lin, "Selective transfer learning for EEG-based drowsiness detection," in *Proc. IEEE Int. Conf. Syst., Man, Cybern. (SMC)*, Oct. 2015, pp. 3229–3232.

[39] J.-R. Duann, P.-C. Chen, L.-W. Ko, R.-S. Huang, T.-P. Jung, and C.-T. Lin, "Detecting frontal EEG activities with forehead electrodes," in *Foundations of Augmented Cognition. Neuroergonomics and Operational Neuroscience*, D. D. Schmorrow, I. V. Estabrooke, and M. Grootjen, Eds. Berlin, Germany: Springer, 2009, pp. 373–379.

[40] J. Onton, M. Westerfield, J. Townsend, and S. Makeig, "Imaging human EEG dynamics using independent component analysis," *Neurosci. Biobehavioral Rev.*, vol. 30, no. 6, pp. 808–822, 2006.

[41] C.-T. Lin *et al.*, "Tonic and phasic EEG and behavioral changes induced by arousing feedback," *NeuroImage*, vol. 52, no. 2, pp. 633–642, 2010.

[42] Y.-T. Wang *et al.*, "Developing an EEG-based on-line closed-loop lapse detection and mitigation system," *Frontiers Neurosci.*, vol. 8, p. 321, Oct. 2014.

[43] B. J. Lance, S. E. Kerick, A. J. Ries, K. S. Oie, and K. McDowell, "Brain–computer interface technologies in the coming decades," *Proc. IEEE*, vol. 100, no. Special Centennial Issue, pp. 1585–1599, May 2012.

[44] *EEG Headsets | NeuroSky Store*. Accessed: Sep. 22, 2016. [Online]. Available: http://Neurosky.com and http://store.neurosky.com/

[45] Muse. *Muse—Muse: The Brain Sensing Headband*. Accessed: Sep. 22, 2016. [Online]. Available: http://store.choosemuse.com/products/muse?_ga=1.40886502.570081481.1474579055

[46] *EMOTIV EPOC+ 14 Channel Mobile EEG—Emotiv*. Accessed: Sep. 22, 2016. [Online]. Available: https://www.emotiv.com/product/emotiv-epoc-14-channel-mobile-eeg/ and https://Emotiv.com

[47] S. Xu *et al.*, "Soft microfluidic assemblies of sensors, circuits, and radios for the skin," *Science*, vol. 344, no. 6179, pp. 70–74, Apr. 2014.

[48] E. Werth, P. Achermann, D.-J. Dijk, and A. A. Borbély, "Spindle frequency activity in the sleep EEG: Individual differences and topographical distribution," *Electroencephalogr. Clin. Neurophysiol.*, vol. 103, no. 5, pp. 535–542, Nov. 1997.

[49] I. Tavor, O. P. Jones, R. B. Mars, S. M. Smith, T. E. Behrens, and S. Jbabdi, "Task-free MRI predicts individual differences in brain activity during task performance," *Science*, vol. 352, no. 6282, pp. 216–220, Apr. 2016.